# Reactor Relevant Current Drive and Heating by N-NBI on JT-60U

T. Oikawa 1), Y. Kamada 1), A. Isayama 1), T. Fujita 1), T. Suzuki 1), N. Umeda 1),
M. Kawai 1), M. Kuriyama 1), L.R. Grisham 2), Y. Ikeda 1), K. Kajiwara 1) , K. Ushigusa 1),
K. Tobita 1), A. Morioka 1), M. Takechi 1), T. Itoh 1) and the JT-60 TEAM
1) Japan Atomic Energy Research Institute, Naka Fusion Research Establishment,
2) Princeton Plasma Physics Laboratory,

e-mail contact of main author: toikawa@naka.jaeri.go.jp

**Abstract.** Current drive capability of negative-ion-based NBI (N-NBI) in JT-60U has been extended to the reactor relevant regime. Driven current profile and current drive efficiency have been evaluated in the high temperature regime of central electron temperature $T_e(0) \sim 10 \text{keV}$, and reasonable agreement with theoretical prediction has been confirmed in this regime. N-NB driven current reached 1MA with injection power of 3.75MW at beam energy of 360keV. The current drive efficiency of $1.55 \times 10^{19} \text{Am}^{-2}\text{W}^{-1}$ approaching to the ITER requirement was achieved in the high $\beta_p$ H mode plasma with $T_e(0) \sim 13 \text{keV}$. This current drive performance realized the sustainment of high beta ($\beta_N = 2.5$) and high confinement ($\text{HH}_{y2} = 1.4$) plasma in full current-driven condition at the plasma current of 1.5MA. The influence of instabilities on N-NB current drive was studied. When a burst like instability driven by N-NB occurred in the central region, reductions in loop voltage near magnetic axis and neutron production rate due to loss of beam ions were observed although the lost driven current was at most $\sim 7\%$ of the total driven current. When neoclassical tearing instability appeared in high beta plasmas, loss of beam ions was enhanced with increasing activity of instability and depended on the location of instability.

## 1 Introduction

Non-inductive current drive is an essential issue for steady-state operation of tokamak fusion reactor. Neutral beam injection (NBI) is one of the most promising methods for heating and current drive because the physics of NB has almost been understood and NB has the robustness against edge plasma condition. To study heating and current drive by high energy beam, negative-ion-based NBI (N-NBI) system with design values of 500keV and 10MW has been installed in JT-60U [1] and its operation has been started in 1996 [2]. Presently, further improvement and optimization of N-NBI system is continued [3]. The fundamental physics related with high energy neutral beam, i.e., the multistep ionization process and current drive capability, have been made clear [4]. This paper describes progress in N-NB current drive capability and influence of instabilities on N-NB current drive. In section 2, current drive characteristics in electron temperature regime of $\sim 10 \text{keV}$ and achievement of highest NB current drive efficiency are presented. Influences of beam driven instability and neoclassical tearing mode on current drive are discussed in section 3. Finally, the main conclusions are summarized in section 4.

## 2 Reactor Relevant Current Drive

As already reported, the current profile driven by high energy neutral beam has been experimentally identified and agreed with the theoretical prediction, and current drive efficiency was increased with electron temperature and beam energy [4]. In these former results, however, plasma temperature was relatively low ($T_e(0) \lesssim 5 \text{keV}$). To increase reliability in the design for ITER and prospect for the future reactor use, evaluation of N-NB current drive capability in higher electron temperature regime has been conducted as reported in section 2.1. In section 2.2, achievement of current drive efficiency approaching to the ITER regime in the full-current-driven condition and progress in N-NB current drive capability are presented.

## 2.1 Current Drive in High Temperature Regime

In order to evaluate N-NB driven current in high electron temperature regime of $T_e(0) \sim 10\text{keV}$, we adopted newly installed ECRF [5]. A low density L mode plasma was employed for precise measurement of N-NB driven current. Non-inductive current other than that driven by N-NB has to be minimized for accurate measurement of N-NB driven current profile because N-NB driven current profile is evaluated by subtracting bootstrap current and driven current by other methods such as positive ion based NBI (P-NB) from total non-inductive current profile which is a directly measurable quantity. Bootstrap current is small in the low density L mode plasma. Co- and counter-directional tangential P-NBIs have been balanced. Figure 1 shows typical discharge waveforms of the experiments. Plasma current and toroidal magnetic field were 1.2MA and 3.73T, respectively. The line-averaged density in the central chord
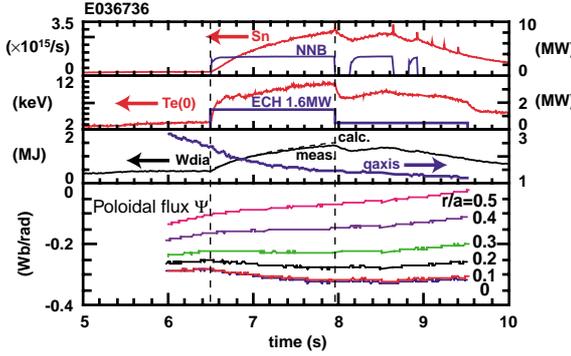


FIG 1: Waveforms of pulse E036736. Injection powers of N-NB and ECH, neutron production rate $S_n$, central electron temperature $T_e(0)$, measured and simulated stored energy $W_{\text{dia}}$, safety factor on axis $q_{\text{axis}}$ and poloidal flux at $r/a = 0 \sim 0.5$ are shown.
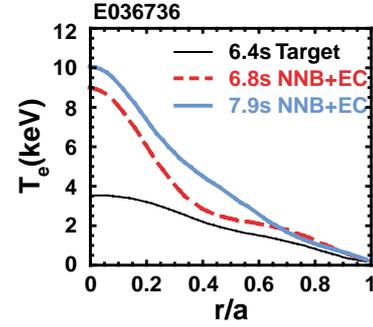
FIG 2: Electron temperature $T_e$ profiles at t=6.4, 6.8 and 7.9sec.

was kept $0.74 \times 10^{19}\text{m}^{-3}$. Injection of N-NB ($E_B$ : 360keV, $P_{\text{INJ}}$ : 3.75MW) and EC wave ($f_{\text{EC}}$ : 110GHz, $P_{\text{EC}}$ : 1.6MW) started at t=6.5s. Central electron temperature $T_e(0)$ was raised to $\sim 8\text{keV}$ rapidly by ECRF, and gradually increased up to 10keV with a time constant of slowing-down time of N-NB fast ions ($\sim 3\text{s}$). Figure 2 shows time evolution of electron temperature profiles at timings of target (t=6.4s), initial phase of N-NB and ECRF (t=6.8s) and end of N-NB and EC injection phase. At t=6.8s, a strongly peaked electron temperature was formed due to a narrow power deposition of ECRF at the plasma center. At =7.9s, higher and broader $T_e$ profile with a central value of 10keV was obtained. Diamagnetic stored energy $W_{\text{dia}}$ and neutron production rate $S_n$ also increased in time scale of slowing-down time of N-NB ions.

Time evolution of reconstructed poloidal flux from magnetic axis to half minor radius are also shown in Fig. 1. Positive and negative slope of each trace corresponds to positive and negative loop voltage at each location, respectively. During t=6.5-7.96s, loop voltage inside r/a=0.4 became negative, which means current was overdriven by large non-inductive current of N-NB and ECRF. At t=7.96s, 2 gyrotrons of ECRF system stopped and ECRF power decreased down to 0.5MW. Magnitude of negative loop voltage became smaller due to reduction of EC driven current and partially to reduction of N-NB current drive caused by decrease in electron temperature. Non-inductive current profile was analyzed at the end of 1st pulse of N-NB(t=7.9s) in the manner in Ref. [6]. Figure 3 shows N-NB driven current profile $J_{\text{NNB}}$ by the measurement (solid line) and the theoretical prediction (dashed line). Shaded region indicates error in measured
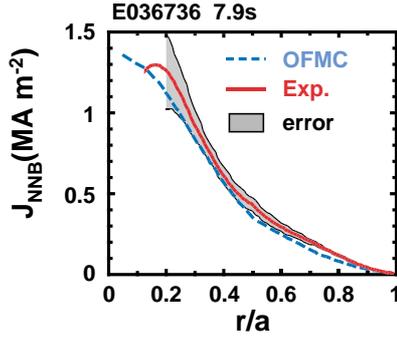
FIG 3: Comparison of $J_{\mathrm{NNB}}$(exp.) with $J_{\mathrm{NNB}}$(OFMC). Both agrees within uncertainty indicated by shaded region.
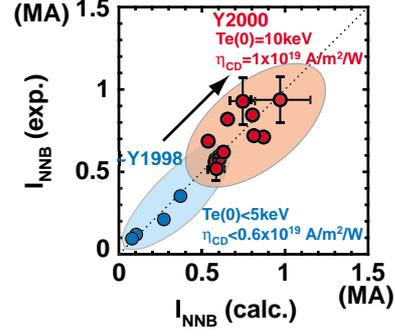
FIG 4: Comparison of N-NB driven current $I_{\mathrm{NNB}}$(exp.) with $I_{\mathrm{NNB}}$(calc.) shows an agreement over a wide range from 0.1MA to 1MA.

profile due to uncertainties in profiles of temperature, density and effective charge, $V_{\mathrm{loop}}$ and estimation of the EC driven current. Theoretical result was calculated by Orbit Following Monte Carlo (OFMC) code. N-NB fast ions built up to 84% to the steady-state in 1.45s injection from comparison of time evolution of measured $W_{\mathrm{dia}}$ with that calculated by OFMC as shown in Fig. 1. Thus, profile by theoretical calculation in Fig. 3 was regulated to 84% to the steady-state solution of OFMC. Experimentally determined and theoretically calculated profiles of N-NB driven current profile agrees within uncertainty. Experimentally measured N-NB driven current reached up to 1MA, a record value of NB current drive in JT-60U. Corresponding current drive efficiency $\eta_{\mathrm{CD}}$ was $1 \times 10^{19} \mathrm{Am}^{-2}\mathrm{W}^{-1}$. Figure 4 shows comparison of experimentally measured N-NB driven current with the calculated one in the range of 0.1 - 1MA. Confirmation of N-NB current drive capability with high accuracy over a wide range of electron temperature reaching $\sim$10keV and $\eta_{\mathrm{CD}} \sim 1 \times 10^{19} \mathrm{Am}^{-2}\mathrm{W}^{-1}$ shows validity of theoretical prediction and gives more confidence to the design of high energy neutral beam for ITER.

## 2.2 Achievement of Current Drive Efficiency approaching to the ITER regime

By using the ECRF system for higher electron temperature and the newly developed stored energy feedback control [7] for stability in high beta regime, full non-inductive current drive at $I_{\mathrm{p}} = 1.5$MA and the ITER relevant value of the N-NB current drive efficiency $1.55 \times 10^{19} \mathrm{Am}^{-2}\mathrm{W}^{-1}$ were achieved. The discharge waveforms are shown in figure 5. N-NB (360keV, 4MW) was injected into the high $\beta_{\mathrm{p}}$ H mode plasma formed by P-NB injection (80-85keV, 20MW). Stored energy was kept around 5.5MJ corresponding to $\beta_{\mathrm{N}} \sim 2.5$ by the stored energy feedback control scheme for avoidance of beta collapse and neoclassical tearing instability which appears in high beta discharge [8]. In advance to N-NB injection , EC wave of 1.5MW was injected in order to raise electron temperature for effective N-NB current drive. After flattop of stored energy at t=5.5s, electron temperature still continued to increase due to the N-NB electron heating in timescale of slowing-down time ($\sim$1.2 s). On the other hand, ion temperature was almost kept constant after formation of high $\beta_{\mathrm{p}}$ mode at t=5s. Figure 6 shows profiles of ohmic current and non-inductive currents by N-NB, P-NB and bootstrap current calculated by ACCOME code at t=6.4s. Driven currents by N-NB, P-NB and ECRF and bootstrap current are 608kA, 255kA, 53kA and 760kA, respectively. Current drive efficiency of the N-NB reached the record value for neutral beam current drive $1.55 \times 10^{19} \mathrm{Am}^{-2}\mathrm{W}^{-1}$, where $T_{\mathrm{e}}(0)$, the line-average density in the central chord and the effective charge $Z_{\mathrm{eff}}$ was $\sim$13keV, $3.05 \times 10^{19}\mathrm{m}^{-3}$ and 3. Total non-inductive current reached 1.68MA over plasma current of 1.5MA. Simultane-
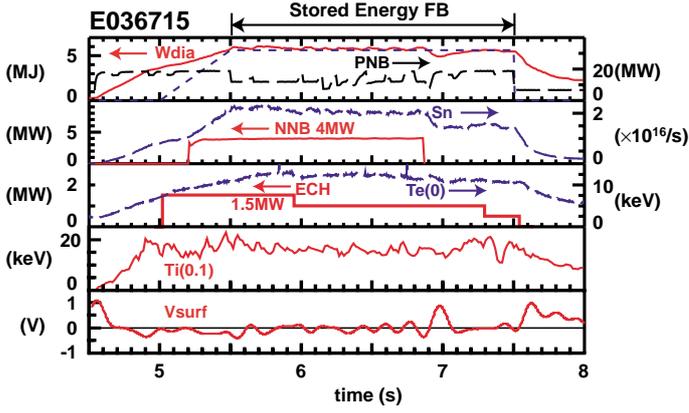
FIG 5: Waveforms of pulse E036715 in which the highest $\eta_{CD}$ was achieved. Diamagnetic stored energy $W_{dia}$ and its reference value for the stored energy feedback control, injection powers of N-NB, P-NB and ECRF, neutron production rate $S_n$, central electron temperature $T_e(0)$, ion temperature near axis (r/a=0.1) $T_i(0.1)$, and surface loop voltage $V_{surf}$ are shown.
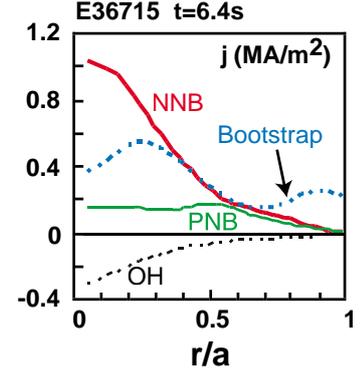
FIG 6: Profiles of driven currents by N-NB, P-NB, bootstrap current and ohmic current at t=6.4s calculated by ACCOME code.

ously, high core-plasma performance of $\beta_N = 2.5$ and $HH_{y2} = 1.4$ was achieved.

Result of N-NB current drive performance reaching $1.55 \times 10^{19} \mathrm{Am}^{-2}\mathrm{W}^{-1}$ is a steady-state solution by ACCOME code. Thus, to confirm this result, the discharge was analyzed by time-dependent transport code TOPICS. Figure 7 shows time evolution of non-inductive current by N-NB, P-NB, ECRF and bootstrap current with a level of $I_p = 1.5\mathrm{MA}$. N-NB driven current and bootstrap current evolve in time, and the fully non-inductively current driven condition was reached at t=5.8s. Non-inductive current fully built up at t=6.5s. Values of non-inductive currents estimated by TOPICS code are consistent with those of the steady-state solution by ACCOME code. In Fig. 7, calculated time evolutions (bold line) of surface loop voltage $V_{surf}$, neutron production rate $S_n$, diamagnetic stored energy $W_{dia}$ and central safety factor are compared to the measurements (thin line). Calculated time evolutions of these quantities are consistent with the experimental time traces. Thus, achievement of highest current drive efficiency can be certainly confirmed.

Figure 8 shows the progress in the N-NB current drive capability. As shown in $\eta_{CD}$-$T_e(0)$ plot (Fig. 8 (a)), $\eta_{CD}$ has been confirmed to increase with electron temperature over 10 keV approaching to the ITER regime. High values of current drive efficiency larger than $1 \times 10^{19} \mathrm{Am}^{-2}\mathrm{W}^{-1}$ obtained at $T_e(0) > 8\mathrm{keV}$ were achieved in a series of large driven current experiments described in section 2.1 and high $\beta_p$ H mode plasmas described in this section. Here, the range of N-NB beam energy is 330-370 keV, and $Z_{eff}$ is from 2 to 4. In Fig. 8 (b), $\eta_{CD}$ is plotted versus driven current $I_{NB}$. Simultaneous achievement of $\eta_{CD} = 1 \times 10^{19} \mathrm{Am}^{-2}\mathrm{W}^{-1}$ and $I_{NB} = 1\mathrm{MA}$ indicates an advantage of high energy neutral beam in current drive.

## 3 Influence of Instabilities on N-NB Current Drive

The conclusion of validity of theoretical prediction for N-NB current drive described in section 2 was for MHD-quiescent plasmas. However, various instabilities such as sawtooth, beam driven instability and neoclassical tearing mode appear in tokamak plasma. In this section, influence of instabilities on N-NB current drive is investigated.
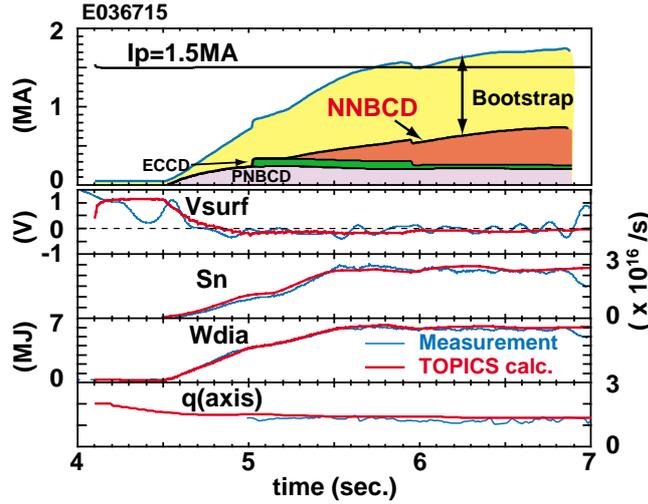
FIG 7: Time evolutions of non-inductive currents by N-NBCD, P-NBCD, ECCD and bootstrap current calculated by time-dependent transport code for pulse E036715. Calculated time evolutions (bold line) of surface loop voltage $V_{\text{surf}}$, neutron production rate $S_{\text{n}}$, diamagnetic stored energy $W_{\text{dia}}$ and central safety factor are compared to the measurements (thin line).
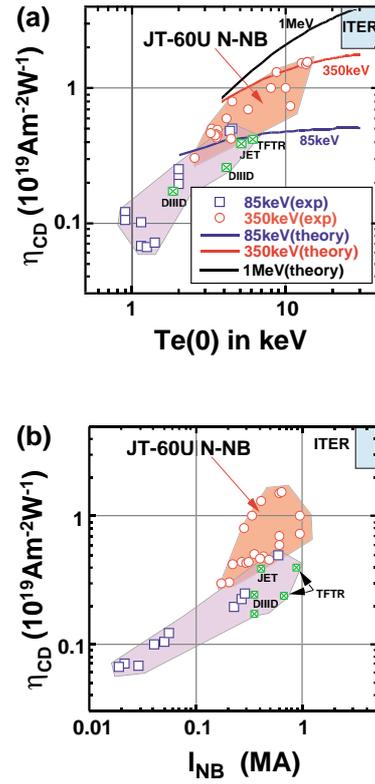


FIG 8: (a) $T_{\text{e}}$ dependence of current drive efficiency $\eta_{\text{CD}}$, and (b) $\eta_{\text{CD}}$ versus driven current $I_{\text{NB}}$ for N-NB(330-370keV) and P-NB(85keV). Data of TFTR, JET and DIII-D have been taken from Ref. [9], [10] and [11].

## 3.1 Beam Driven Instability

In the low density plasmas with beam pressure of N-NB comparable to thermal pressure, a burst-like instability sometimes appeared. Figure 9 (a) shows the waveforms of the discharge such instability appeared. Toroidal magnetic field was 3.73T, and the line-averaged density in the central chord was $0.65 \times 10^{19}\text{m}^{-3}$. As shown in the time trace of $S_{\text{n}}$, N-NB ions built up gradually ($\sim 90\%$ in 1 second injection). Frequency spectrum of magnetic fluctuation measured by Mirnov coils is also shown in Fig. 9 (a). Small bursts with frequency of 60-80 kHz appeared after start of N-NB injection, and their range of frequency sweeping gradually became wider. At t=7.96s when a large burst indicated as 1st burst in the figure occurred, reduction in $S_{\text{n}}$ was observed. This means losses of thermal ions and/or fast ions of P-NB and/or N-NB. Time traces of reconstructed poloidal flux inside $r/a < 0.4$ is also shown in Fig. 9 (a). Slopes inside $r/a \leq 0.3$ increased from t=7.96s (1st burst). This means that non-inductive current in the central region were lost by this burst. In this discharge, bootstrap current and P-NB current drive were negligibly small because of low pressure and $\beta_{\text{p}}$ and balanced injection of tangential P-NB. Reduction in $T_{\text{e}}$ of $\sim 7\%$ was too small to explain increase in loop voltage. Thus, it can be considered that reduction in non-inductive current was caused by loss of N-NB fast ions carrying current. In Fig. 9 (b), $T_{\text{e}}$ measured by ECE at $r/a = 0.3$ for t=7.9-8.2s are shown. Increase in signals corresponding to 1st, 2nd and 3rd bursts were observed. This suggests that
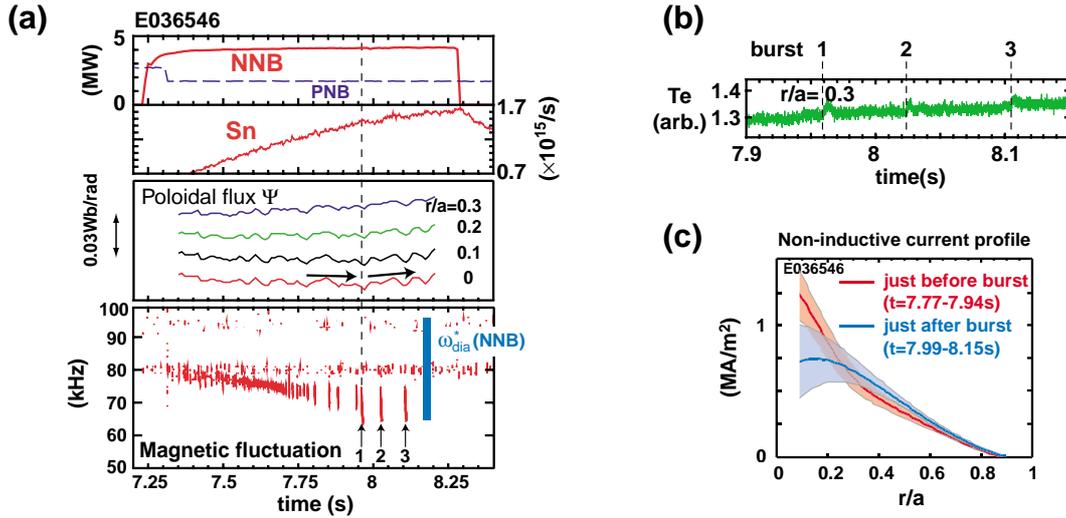
*FIG* 9: (a) Waveforms of pulse E036546. Injection powers of N-NB and P-NB and $S_\mathrm{n}$ are shown in 1st panel. Time evolutions of reconstructed poloidal flux at r/a = 0 - 0.4 and frequency spectrum of magnetic fluctuation are also shown. (b) Crashes in $T_\mathrm{e}$ measured by ECE corresponding to 1st-3rd magnetic bursts in (a). (c) Measured non-inductive current profile just before and after 1st magnetic burst. Shaded regions correspond to the errors in each profiles.

instability occurred inside $r/a = 0.3$, which is consistent with the reduction in loop voltage inside $r/a \sim 0.3$. No clear change in $S_\mathrm{n}$ and poloidal flux was observed for bursts before 1st burst. Toroidal mode number of these bursts was n=1. Central safety factor $q_\mathrm{axis}$ was $\sim 1.5$, and safety factor at r/a=0.3 was $\sim 2$. Thus, if this instability inside r/a=0.3 was TAE mode, poloidal mode number would be m=1. However, corresponding TAE frequency is 380kHz far larger than the observed frequency of $60-80$kHz. In addition, the ratio of velocity of N-NB ions parallel to magnetic field $v_{\mathrm{b}//}$ to Alfvén velocity $v_\mathrm{A}$, $v_{\mathrm{b}//}/v_\mathrm{A}$, is 0.2 less than even the side-band resonant conditions of $\sim 0.3$ for TAE mode and $\sim 0.5$ for GAE mode. Thus, it is difficult to explain this instability by AE mode although a burst like behavior was similar to the Frequency sweeping mode (considered TAE mode) as described in [12]. As shown in the frequency spectrum of magnetic fluctuation (Fig. 9 (a)), diamagnetic drift frequency of N-NB fast ions $\omega_\mathrm{dia}^*$ for m=2 mode inside r/a=0.3 is estimated to be 64-96kHz from OFMC calculation, while diamagnetic drift frequency of thermal ions is less than 3kHz. Thus, frequency of this burst-like instability was determined by the diamagnetic drift frequency of N-NB fast ions. Classification of this instability is still open question.

To evaluate the influence of this instability on N-NB current drive, non-inductive driven current profiles just before and after 1st burst were analyzed as in Fig. 9 (c). Non-inductive current inside $r/a < 0.3$ decreased after a burst. Because periods for analysis could not be taken long enough for accurate determination of loop voltage profiles, maximum difference between non-inductive current profiles before and after instability has been estimated. Shaded regions correspond to the errors in each profiles. Lost driven current of N-NB inside $r/a < 0.3$ was estimated in maximum to be $\sim 40$kA corresponding to 7% of total N-NB driven current. In almost cases in other discharges with similar instabilities, clear influence on plasma as in the case mentioned here was not observed. Thus, reduction in N-NB driven current was not serious in present experiments. However, with higher beam pressure and different safety factor profile, there is a possibility that degradation of current drive caused by the instability can not be negligible.

## 3.2　Tearing Mode in High Beta Plasma

In high beta discharges, neoclassical tearing instability appears when $\beta_N$ reaches onset level. Reduction of the neutron production rate $S_n$ or saturation of its increase were observed during the instability. Figure 10 shows waveforms of discharge which tearing mode with poloidal and
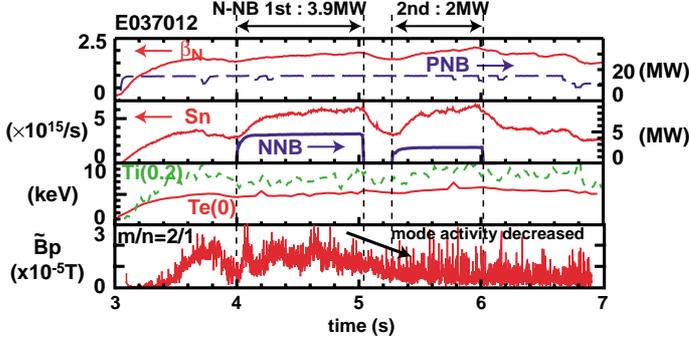


*FIG* 10: Waveforms of pulse E037012. Neoclassical tearing mode with m/n=2/1 appeared. $\beta_N$, injection powers of N-NB and P-NB, $S_n$, $T_e(0)$, $T_i(0.2)$, and magnetic fluctuation (n=1) are shown.
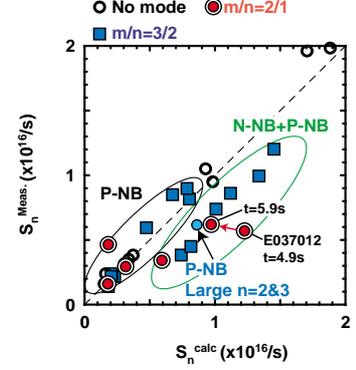
*FIG* 11: Comparison of the measured $S_n$ to the calculated values. No tearing mode, m/n=2/1, m/n=3/2 and n=3 are shown.

toroidal mode number m/n=2/1 appeared. At t=3.4s, m/n=2/1 mode with large activity appeared and was sustained till t=5s. Small n=2 mode also existed. Amplitude of magnetic fluctuation decreased after t=5s. N-NB of 4MW was injected during large activity (t=4-5s), and after short break, 2MW was injected during weak activity phase (t=5.3-6s). Ion temperature at $r/a = 0.2$, $T_i(0.2)$, started to increase gradually after decrease in tearing mode activity. Central electron temperature $T_e(0)$ continued to increase after decrease in tearing mode activity in spite of half injection power of N-NB. Saturated value of $S_n$ for 2nd N-NB pulse (2MW) was higher than for 1st pulse (4MW) during large tearing activity. This difference can not be explained only by difference of temperature and density.

In Fig. 11, measured $S_n$ are compared to the calculated values by the transport code with taking into consideration the orbit, ripple and charge exchange losses evaluated by OFMC code. Data for no instability, m/n=3/2, m/n=2/1 and n=3 tearing modes are shown. Measured values agree with the calculated values for no mode cases. For only P-NB injection cases, the differences between measurement and calculation are not large. The differences are larger for cases of N-NB and P-NB injection. This suggests that N-NB ions suffered larger transport than P-NB ions. Reduction for 2/1 mode are larger than for 3/2 mode. This may be due to following facts. Tearing mode with m/n=2/1 locates at $r/a \sim 0.2$ where large portion of N-NB fast ions are deposited and radial location of 3/2 mode is $r/a \sim 0.5$ outside the peak of N-NB deposition (3/2 and 2/1 modes appeared in different discharge scenario). Even for only P-NB injection case, the measured $S_n$ became less than the calculated value clearly when two modes (n=2 and n=3) with large activity coexisted, as shown in the figure. This suggests that tearing instability causes loss or redistribution of beam ions. In DIII-D, reduction in driven current by P-NB during tearing modes was observed [13]. Thus, loss mechanism of circulating beam ions has to be understood through modelling, and suppression of neoclassical tearing mode [14] is necessary for effective current drive and heating by N-NB.

## 4 Conclusion

In JT-60U, current drive by N-NB has been comprehensively studied to demonstrate applicability and effectiveness of high energy neutral beam for current drive as follows.
· Current drive characteristics have been investigated over a wide range of $T_e$ $(3 - 10\text{keV})$, and reasonable agreement with theoretical prediction has been confirmed.
· N-NB driven current reached $1\text{MA}$ with injection power of 3.75MW at $T_e(0) = 10\text{keV}$. Corresponding current drive efficiency was $1 \times 10^{19}\text{Am}^{-2}\text{W}^{-1}$
· The record value of the NB current drive efficiency $1.55 \times 10^{19}\text{Am}^{-2}\text{W}^{-1}$ approaching to the ITER requirement was achieved at $T_e(0) \sim 13\text{keV}$. High beta $(\beta_N = 2.5)$ and high confinement $(\text{HH}_{y2} = 1.4)$ plasma has been also sustained in full current-driven condition at $I_p$=1.5MA. The influence of instabilities on N-NB current drive was studied.
· A beam driven burst-like instability appeared in the central region of the low density plasma with beam pressure of N-NB comparable to thermal pressure. N-NB fast ions carrying non-inductive current were lost in the center $(r/a < 0.3)$. Decrease in the driven current was at most $\sim 7\%$ of the total driven current.
· When neoclassical tearing instability appeared, reduction of $S_n$ suggests loss or redistribution of fast ions. Loss for N-NB ions was larger than that for lower energy beam. Loss of beam ions was enhanced with increasing activity of instability. Beam ions were affected more largely when mode location coincides beam deposition.

## Acknowledgements

## References

[1] KURIYAMA, M., et al., Fusion Eng. Des. 26(1995)445.

[2] USHIGUSA, K., Proc. 16th Int. Conf.(Montreal,1996), vol.1, IAEA, Vienna (1997)37.

[3] GRISHAM, L.R., et al., IAEA-CN-77/FT/3 and FTP/1/17, this volume.

[4] OIKAWA, T., et al., Nucl. Fusion **40** (2000) 435.

[5] IKEDA, Y.I., et al., IAEA-CN-77/EXP4/03, this volume.

[6] FOREST, C. B., et al., Phys. Rev. Lett. 73 (1994)2444.

[7] OIKAWA, T., JAERI-Research 99-048(1999)15.

[8] KAMADA, Y., et al., Nucl. Fusion **39** (1999) 1845.

[9] Scott, S.D., et al., Proc. 12th Int. Conf.(Nice,1988), vol.1, IAEA, Vienna (1989)655.

[10] Challis, C.D., et al., Nucl. Fusion **29** (1989) 563.

[11] Prater, R., et al., Plasma Phys. Control Fusion, 35(1993)A53.

[12] SHINOHARA, K., et al., IAEA-CN-77/EXP2/05, this volume.

[13] FOREST, C. B., et al., Phys. Rev. Lett. 79 (1997)427.

[14] ISAYAMA, A., et al., IAEA-CN-77/EXP3/03, this volume.